Protoplasma (1995) 189: 229–237

PROTOPLASMA

Microfilament distribution in protonemata of the moss *Ceratodon*

L. M. Walker* and **F. D. Sack**

Department of Plant Biology, The Ohio State University, Columbus, Ohio

Received November 10, 1994
Accepted April 27, 1995

Summary. Microfilaments were visualized in dark-grown protonemata of the moss *Ceratodon* to assess their possible role in tip growth and gravitropism. The relative effectiveness of rhodamine phalloidin (with or without MBS) and of immunofluorescence (using the C4 antibody) was evaluated for actin localization in the same cell type. Using immunofluorescence, microfilaments were primarily in an axial orientation within the apical cell. However, a more complex network of microfilaments was observed using rhodamine phalloidin after MBS pretreatment, especially when viewed by confocal laser scanning microscopy. This method revealed a rich three dimensional network of fine microfilaments throughout the apical cell, including the extreme apex. Although there were numerous internal microfilaments, peripheral microfilaments were more abundant. No major redistribution of microfilaments was detected after gravistimulation. The combination of MBS, rhodamine phalloidin, and confocal laser scanning microscopy preserves and reveals microfilaments remarkably well and documents perhaps the most extensive F-actin network visualized to date in any tip-growing cell.

Keywords: *Ceratodon*; Protonema; Confocal laser scanning microscopy; Microfilament; Actin.

Abbreviations: BSA bovine serum albumin; CLSM confocal laser scanning microscopy; DIC differential interference contrast; DMSO dimethylsulfoxide; EGTA ethylene glycol bis-(β-amino-ethylether) N,N,N′-tetraacetic acid; FITC fluorescein isothiocyanate; MBS-m-maleimidobenzoyl-N-hydroxysuccinimide ester; MEOH methanol; PBS phosphate buffered saline; PFA paraformaldehyde; PIPES piperazine-N,N′-bis-2-ethanesulfonic acid; PMSF phenylmethyl sulfonyl fluoride; RP rhodamine phalloidin.

Introduction

The cytoskeleton appears to play several important roles in tip-growing cells (Steer and Steer 1989, Schwuchow et al. 1990, Sievers et al. 1991). In moss protonemata, inhibitor studies suggest that microtubules are responsible for maintaining the shape of the apex and the direction of outgrowth, whereas microfilaments are necessary for tip extension (Doonan et al. 1988). However, there is limited information on the distribution of microfilaments in the apical dome of moss protonemata (Doonan et al. 1988) and of other tip-growing cells (Tang et al. 1989, Sievers et al. 1991, Harold and Harold 1992).

Visualization of microfilaments in plant cells is fraught with technical difficulties, including the lability of microfilaments in the presence of aldehyde fixatives (Parthasarathy et al. 1985, Seagull et al. 1987). Use of the protein cross-linking agent MBS (Sonobe and Shibaoka 1989) improves the visualization of microfilaments, especially in conjunction with rhodamine phalloidin (RP) and confocal scanning microscopy (Abel et al. 1989, Goode et al. 1993, Liu and Palevitz 1992, Cleary et al. 1992).

Microtubules become redistributed during gravitropism of *Ceratodon* protonemata and microtubules are load-bearing for plastids in these cells (Schwuchow et al. 1990, Schwuchow and Sack 1994). Here we examined microfilament patterns in dark-grown *Ceratodon* protonemata. Limited comparative information exists on the nature of microfilament arrays visualized using MBS/RP or immunofluoresence (Cho and Wick 1991, Harper et al. 1992). Although there have been several studies of moss protonemata using MBS and/or RP (Doonan et al. 1988, Quader and Schnepf 1989), its effectiveness compared to

* Correspondence and reprints: Department of Biology, Indiana University, 142 Jordan Hall, Bloomington, IN 47405, U.S.A

immunofluorescence has not been evaluated. We determined the distribution of microfilaments in vertical and horizontal *Ceratodon* protonemata to understand the possible roles of microfilaments in tip growth and in protonemal gravitropism. In addition, we evaluated which method yielded optimal microfilament visualization in apical and subapical cells.

Material and methods

Plant material

Fragments of light grown protonemata were placed on sterile cellophane overlaying supplemented agar (Walker and Sack 1990) and grown in the dark with the cellophane in a vertical orientation for 5–7 days. This produces hundreds of upright (negatively gravitropic) protonemata. Some plates containing protonemata were rotated 90° and maintained in that orientation for 1.5–3.5 h (Fig. 1).

Rhodamine phalloidin staining

Protonemata were pretreated in position (orientation maintained with respect to gravity) for 20 min in 100 µM of m-maleimidobenzoyl-N-hydroxysuccinimide ester (MBS, Pierce, Rockford, IL, U.S.A.) in PIPES buffer (10–100 mM PIPES, 10 mM EGTA, 5 mM $MgSO_4$ or 5 mM $MgCl_2$, pH 6.8).

This solution was then wicked away with a tissue, and protonemata were then placed flat on slides and stained and mounted in 0.1–0.3 µM rhodamine phalloidin (RP; Molecular Probes Inc., Eugene, OR, U.S.A.) containing 3% methanol (MEOH) for 20–60 min. All steps were performed in dim green light <5 mW/m^2. Stock solutions of MBS (100 mM) and RP (6.6 µM) were dissolved in 100% dimethylsulfoxide (DMSO) and 100% MEOH, respectively. In some trials, protonemata were fixed in place (1–15 min) with freshly prepared paraformaldehyde (PFA; 0.5–4% w/v) prior to, simultaneously, or after MBS treatment. The addition of DMSO, and protease inhibitors such as PMSF (30 µM), leupeptin (50 µg/ml), and pepstatin (14 µM) to any or all of the solutions did not enhance or improve the number of apical cells exhibiting microfilaments, nor did the use of detergents such as Triton X-100 and Nonidet P40. Thus in later experiments these were omitted. Increasing the incubation time and/or concentrations of MBS and rhodamine phalloidin did not improve the quality or number of protonemata with microfilament arrays. No microfilament arrays were observed if cells were treated only with RP in 3% MEOH. 225 vertical protonemata and 140 gravistimulated protonemata stained by RP were analyzed. Of these, 29% of the vertical and 39% of gravistimulated protonemata were analyzed with confocal microscopy.

Immunofluorescence

Protonemata were pretreated in position with 100 µM MBS in 100 mM PIPES buffer for 30–60 min, rinsed in buffer and then fixed 1–7 min in 1–3% PFA. Cells were then washed in buffer, placed on 0.3% (w/v) polylysine hydrobromide (MW = 70,000–150,000; Polysciences, Warrington, PA, U.S.A.) coated coverslips and submerged in –20 °C MEOH for 10 min. Protonemata were then placed for 10 min in phosphate buffered saline (PBS; 120 mM NaCl, 2.7 mM KCl, 10 mM phosphate buffer, pH 7.0) containing 1% (w/v) bovine serum albumin (BSA; Sigma Chemical Co., St. Louis, MO, U.S.A.). Cell walls were digested with 0.5% pectinase (Sigma), and 0.5% cellulysin Y-C (Seishin Pharmaceutical, Tokyo, Japan), in buffer that contained 50 µg/ml leupeptin and 0.3–0.5 mM phenylmethyl-sulfonyl fluoride (PMSF), for 3–10 min and then rinsed with PBS-BSA. Protonemata were incubated in 25 µg/ml C4 monoclonal antibody against mouse actin (Lessard 1988; ICN Biochemical, Costa Mesa, CA, U.S.A.) and then rinsed in PBS-BSA. Protonemata were then incubated in an FITC-conjugated goat anti-mouse (IgG) secondary antibody (Hyclone, Logan, UT, U.S.A.) diluted 1 : 40 and then washed in PBS-BSA. Protonemata were incubated in primary and secondary antibodies (diluted in PBS-BSA) each for 20–60 min at 37 °C. Cells were mounted in Mowiol and 0.1% paraphenylenediamine (Sigma) to retard fading. Immunofluorescence was observed 12 h later. 90 vertical and 139 gravistimulated protonemata stained by immunofluorescence were analyzed.

Microscopy

Protonemata were viewed with a Zeiss IM 35 inverted microscope equipped for epifluorescence. Actin (FITC) immunofluorescence was examined using a 450–490 nm band pass exciter filter, a 510 nm dichroic beam splitter, and a 515 nm long pass barrier filter. Rhodamine phalloidin fluorescence was examined using a 546 nm band pass exciter filter, a 580 nm dichroic beam splitter, and a 590 nm long pass barrier filter. Most observations employed a Zeiss ×63 Planapo oil immersion objective (NA 1.4).

Immunofluorescence images were recorded on Kodak T-Max P3200 35 mm film that was used at an effective ASA of 800 and processed in Kodak T-Max developer. Rhodamine phalloidin-labelled actin arrays were recorded on Kodak T-Max 400 or Plus X 125 film pushed to ASA 600 using T-Max or Diafine developer. Cells stained with rhodamine phalloidin were also observed with a confocal laser scanning microscope system (CLSM, MRC 600; BioRad Inc., Cambridge, MA, U.S.A.) attached to a Nikon Optiphot microscope using a Leitz ×63 oil immersion objective (NA 1.4). Images were photographed from the monitor using T-Max 100 film and processed in T-Max developer.

Results

Optimization of protocol

Treatment with MBS prior to PFA fixation and staining with rhodamine phalloidin or antibodies resulted in the best preservation of microfilaments in *Ceratodon* protonemata. When utilizing RP, the best microfilament arrays were observed when PFA was omitted from the staining protocol. Using conventional fluorescence microscopy, both rhodamine phalloidin and immunofluorescence were effective in revealing microfilaments in apical (Figs. 2 A–E and 3 G–I) and subapical cells (Figs. 2 A, F and 3 F, K). But in almost all trials, more extensive arrays were seen after rhodamine phalloidin labelling than after immunofluorescence (compare Figs. 2 and 3). Thus, rhodamine phalloidin staining was superior to immunofluorescence in visualizing microfilaments in both the apical and subapical cells of protonemata.

Examination of MBS and rhodamine phalloidin treated cells using confocal microscopy (CLSM) dramati-

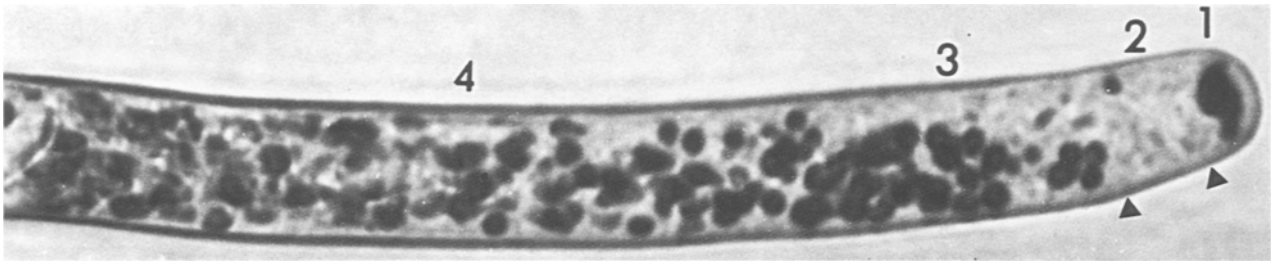

Fig. 1. Dark-grown gravistimulated protonema (1.5 h) demonstrating plastid zonation. Four plastid zones are indicated. Zone 1 contains nonsedimenting amyloplasts. Zone 2 contains no amyloplasts except those in transit between zones 1 and 3. Zone 3 contains large spherical amyloplasts that sediment (small arrows). Zone 4 contains nonsedimenting amyloplasts. The area of microtubule enrichment is within plastid zone 2 and is denoted by arrowheads. ×800. Gravity vector towards bottom of micrograph

cally improved visualization of microfilament number and spatial complexity compared to conventional fluorescence microscopy (compare Figs. 2 and 5). Thus, the best protocol for observing microfilaments in *Ceratodon* protonemata utilized MBS, rhodamine phalloidin, and CLSM. However, this pretreatment with MBS did not maintain the normal longitudinal plastid zonation nor maintain amyloplast sedimentation normally present in horizontal apical cells (Fig. 1). PFA fixation prior to MBS treatment was superior in this regard, but resulted in very poor microfilament preservation. The cold methanol treatment required for immunofluorescence labelling of microfilaments caused amyloplasts to clump together, plasmolysis and flattening of protonemata, and as in RP labelled cells, often resulted in the loss of plastid zonation (Fig. 3 B, J).

Distribution of microfilaments

Apical cells

Using conventional fluorescence microscopy, microfilaments could be seen in apical cells with both rhodamine phalloidin and the C4 antibody (Figs. 2A–E and 3 A, C–E, G–I). However, rhodamine phalloidin routinely produced more extensive labelling of microfilaments than did immunolocalization, and the rhodamine phalloidin method revealed internal as well as peripheral microfilaments (compare Fig. 2 A–E to Fig. 3 A, C–E, G–I).

Using CLSM and MBS/RP, a complex network of microfilaments was visualized which extend throughout the length of the apical cell (Figs. 4 and 5). Microfilaments were closely associated with and surrounded the nucleus (Fig. 4 J–M) and plastids (Fig. 4 E–H). Optical sectioning showed numerous microfilaments in all planes of focus, and microfilaments were fairly uniform in thickness (Fig. 4 A–I). Although there were numerous internal microfilaments, peripheral microfilaments were more abundant (Fig. 4 A–I). There was an extensive array of microfilaments in the very tip of the apex (Figs. 4 and 5).

In contrast, the C4 antibody more often labelled microfilaments that were mostly axial in orientation (Fig. 3 A, E, G–I). It is not clear whether the prominent axial microfilaments visualized with immunofluorescence were not as well preserved using MBS/RP, or whether these axial microfilaments were simply less conspicuous in RP stained cells.

Subapical cells

Subapical cells of *Ceratodon* protonemata usually contained a large central vacuole and microfilaments localized in these cells were mostly peripheral in location and axial in orientation (Figs. 2 A, and 3 F, K). However, some subapical cells did have an extensive internal network of microfilaments, and these networks were observed more often in subapical cells stained with rhodamine phalloidin (Fig. 2 F).

Effects of reorientation

Protonemata were reoriented to the horizontal for 1.5 to 3.5 h, a time sufficient to induce upward gravitropic curvature (Walker and Sack 1990). No difference in microfilament distribution could be detected between vertical and upwardly curving protonemata using either method (compare Fig. 2 A–C to D, E; Fig. 3 A–E to G–I; Fig. 4 A–I to Fig. 5 A–D). No microfilament asymmetry across the cell was observed in any apical cell, regardless of localization protocol, even in regions which become enriched in microtubules in horizontal protonemata (Schwuchow et al. 1990: fig. 1 E).

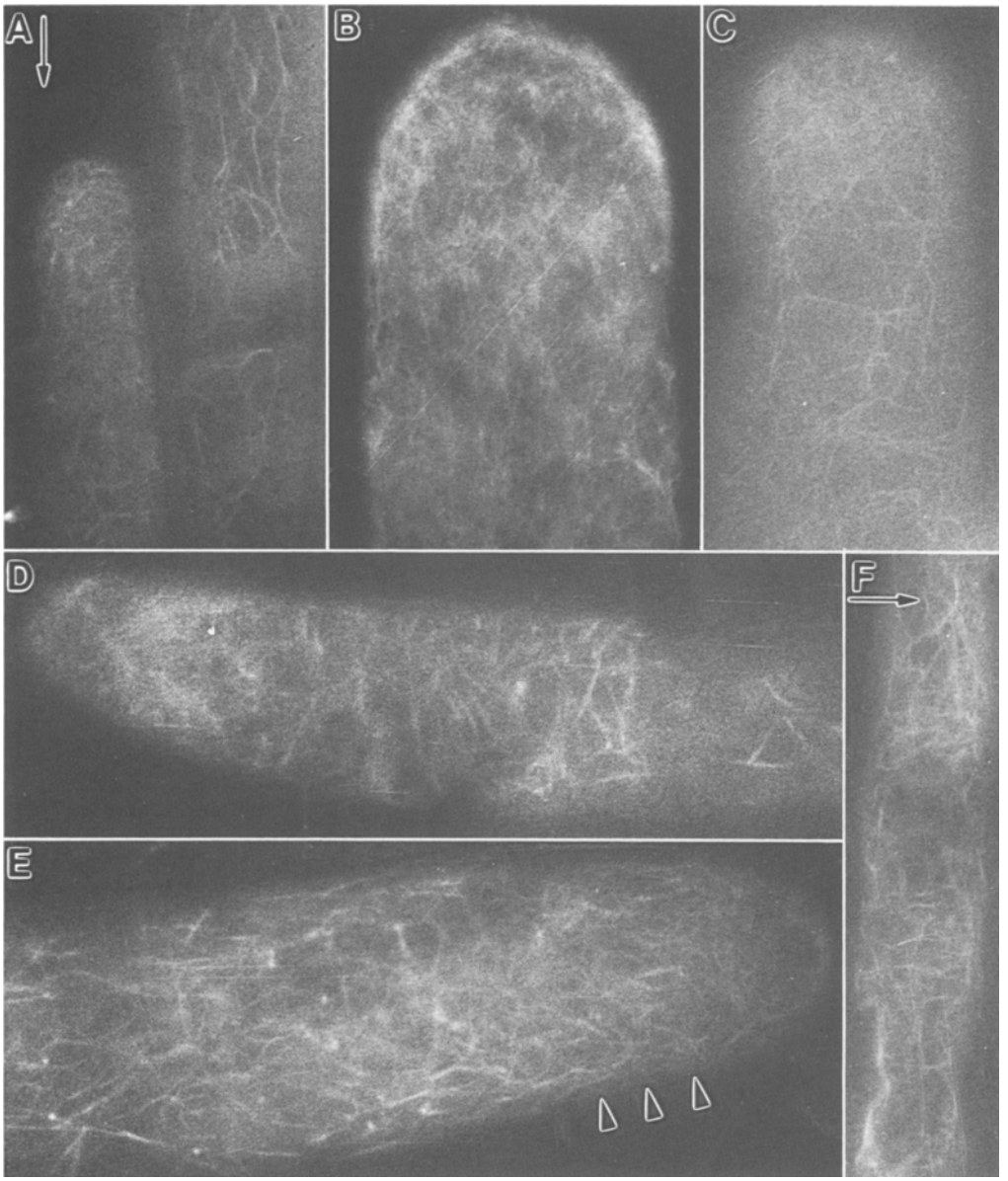

Fig. 2. Rhodamine phalloidin labelling of microfilaments in vertical (**A–C**) and horizontal (**D–F**) dark-grown *Ceratodon* protonemata. Protonemata were observed with conventional fluorescence microscopy. Arrow in **A** indicates direction of gravity vector for **A–E**. **A–C** Vertical protonemata. **A** Apical cell (left) and subapical cell (right); ×700. **B** Apical cell, near median optical section. ×900. **C** Apical cell showing peripheral microfilaments. ×900. **D–F** Protonemata horizontal 1.5 h. **D** Apical cell showing peripheral microfilaments. Cell tip is to left.×1100. **E** Apical cell showing upward curvature and internal microfilaments. Cell tip is to right. Arrowheads indicate areas where microtubule enrichment occurs (Schwuchow et al. 1990) although not shown here. ×1,200. **F** Subapical cell. Arrow indicates direction of gravity vector. ×650

Fig. 3. Immunofluorescence of vertical (**A–F**) and gravistimulated (**G–K**) *Ceratodon* protonemata labelled using the C4 actin antibody and observed with conventional fluorescence microscopy. Arrow indicates direction of gravity vector for **A–J**. All, ×1000. **A–F** Vertical protonemata. **A** Apical cell. Labelled microfilaments are mostly peripheral and axially oriented. **B** Differential interference contrast (DIC) image of field in **A**. Note the vacuolation and clumped amyloplasts. **C** Non-axial peripheral microfilaments in apical cell. **D** Near median optical section of vertical protonema showing internal arrays of fine microfilaments. **E** Axially oriented microfilaments near periphery of apical cell. **F** Subapical cell. **G–K** Protonemata gravistimulated for 3 h. Note predominantly axial orientation of internal (**H**) and peripheral microfilaments (**G** and **I**). **J** DIC image of **I** showing upward curvature of tip. **K** Subapical cell with fine, mostly axially oriented microfilaments. Arrow indicates direction of gravity vector

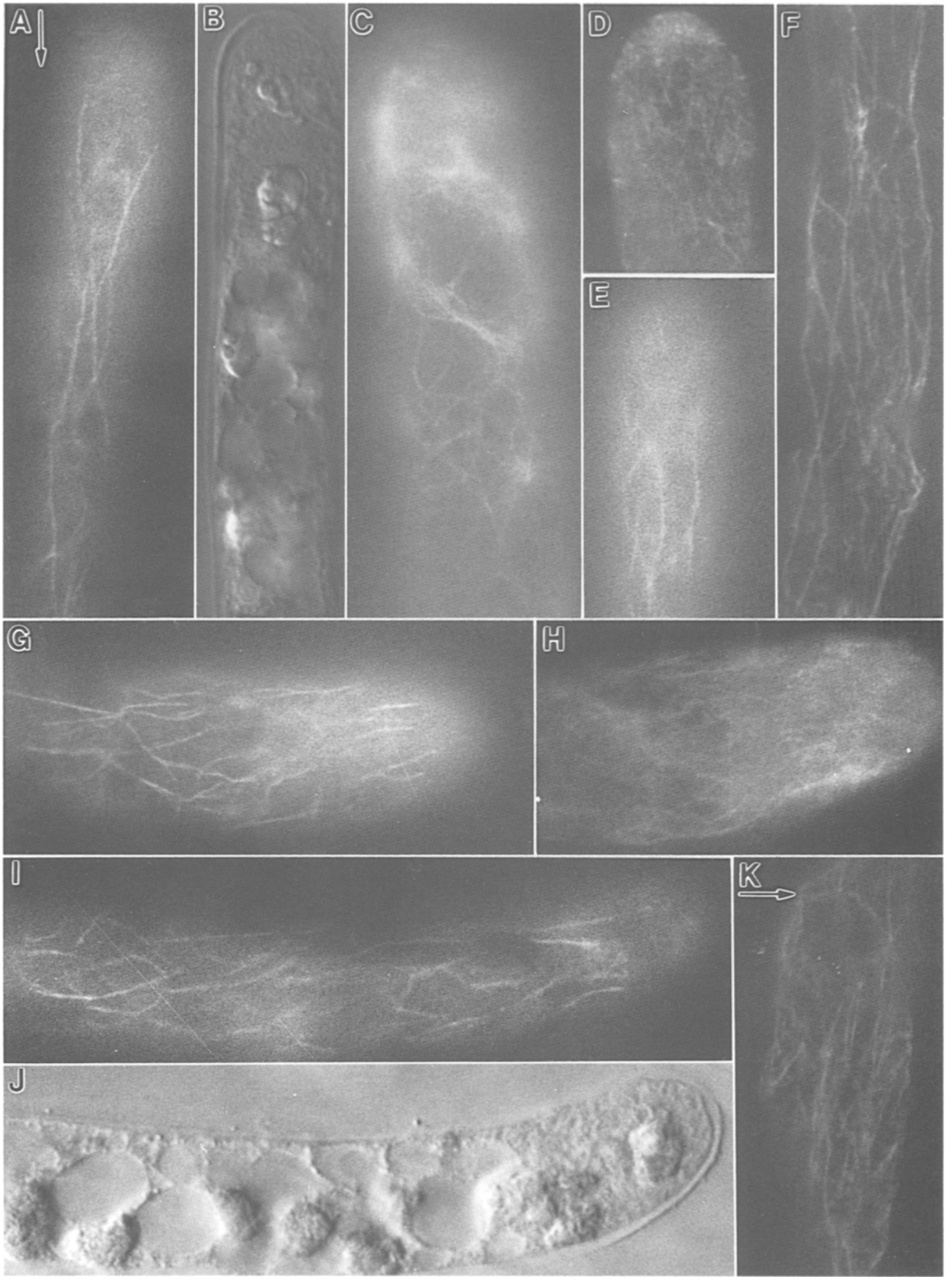
A
B
C
D
E
F
G
H
I
J
K

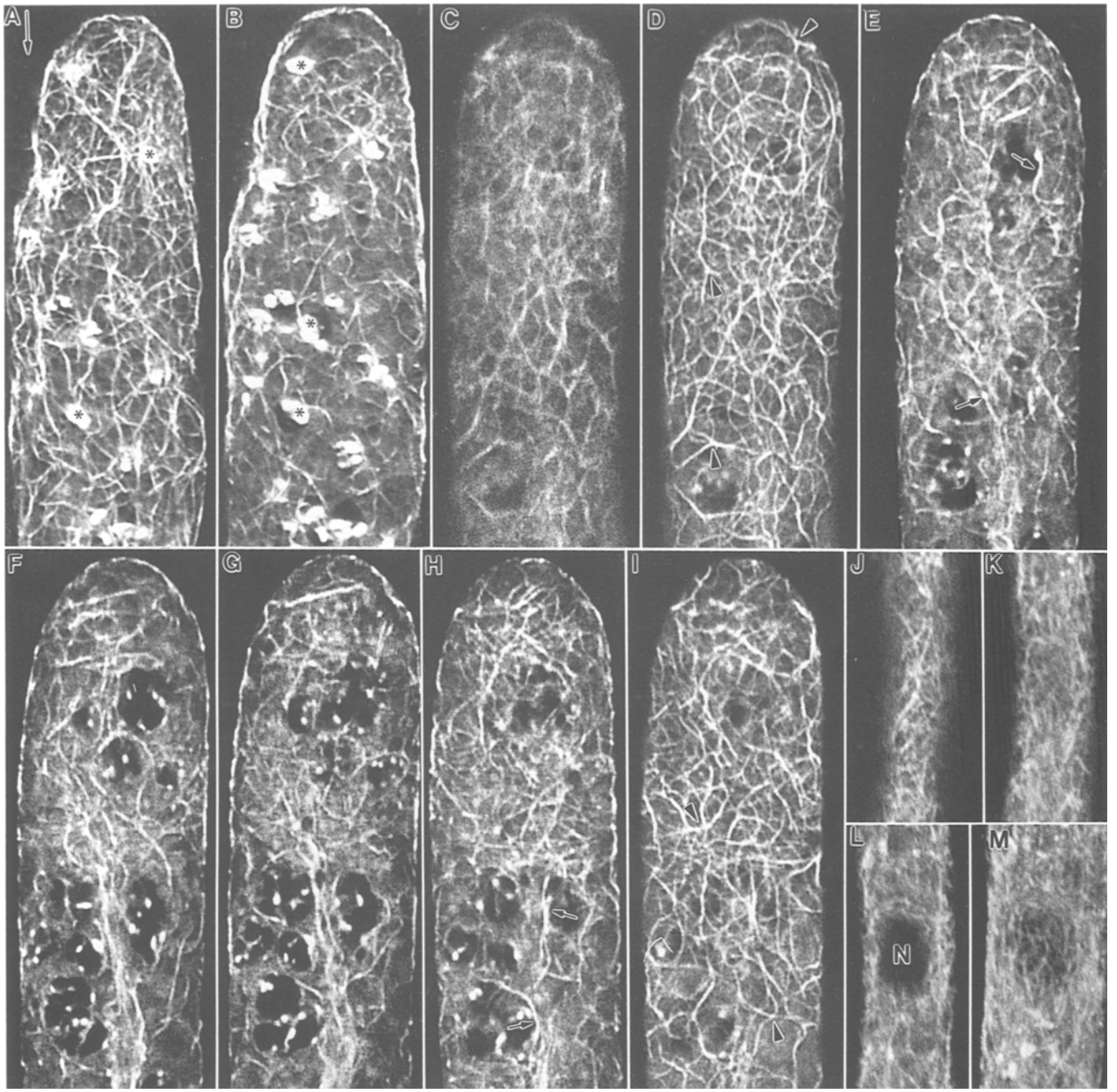

Fig. 4. Rhodamine phalloidin labelling of microfilaments in vertical protonemata observed with confocal laser scanning microscopy. Arrov **A** indicates direction of gravity vector for **A–M**. **A** and **B** Two different optical sections of the same apical cell demonstrating a rich networl peripheral (**A**) and internal (**B**) microfilaments. In **A**, note microfilaments extending into the extreme apex. Bright spots in **A** and **B** (asteri are plastids visualized by autofluorescence of chlorophyll. ×990. **C–I** Serial optical sections (7 in 1 µm intervals) from a single apical c Apparent junctions (branches?) of microfilaments are indicated by arrowheads in **D** and **I**. **C** Microfilaments near to or just under the plas membrane. **D** and **I** Peripheral although more internal than **C**. Note the rich network of microfilaments included in the dome. **E** and **H** Note proximity of plastids and microfilaments (short arrows). Plastids in **C–I** appear to lack any chlorophyll and are detectable more by an abse of fluorescence. **F** and **G** Near median sections. Note the abundance of internal microfilaments, although there are fewer than in the periph of the cell (cf. **D** and **I**). ×990. **K** and **L** Optical sections of nuclear region in apical cell. **J**, **K**, and **L** are 1, 4, and 6 µm deep, respectively, i a cell that is 14 µm thick. **M** Collective projected image of 14 optical sections that are each 1 µm thick. *N* Nucleus; ×750

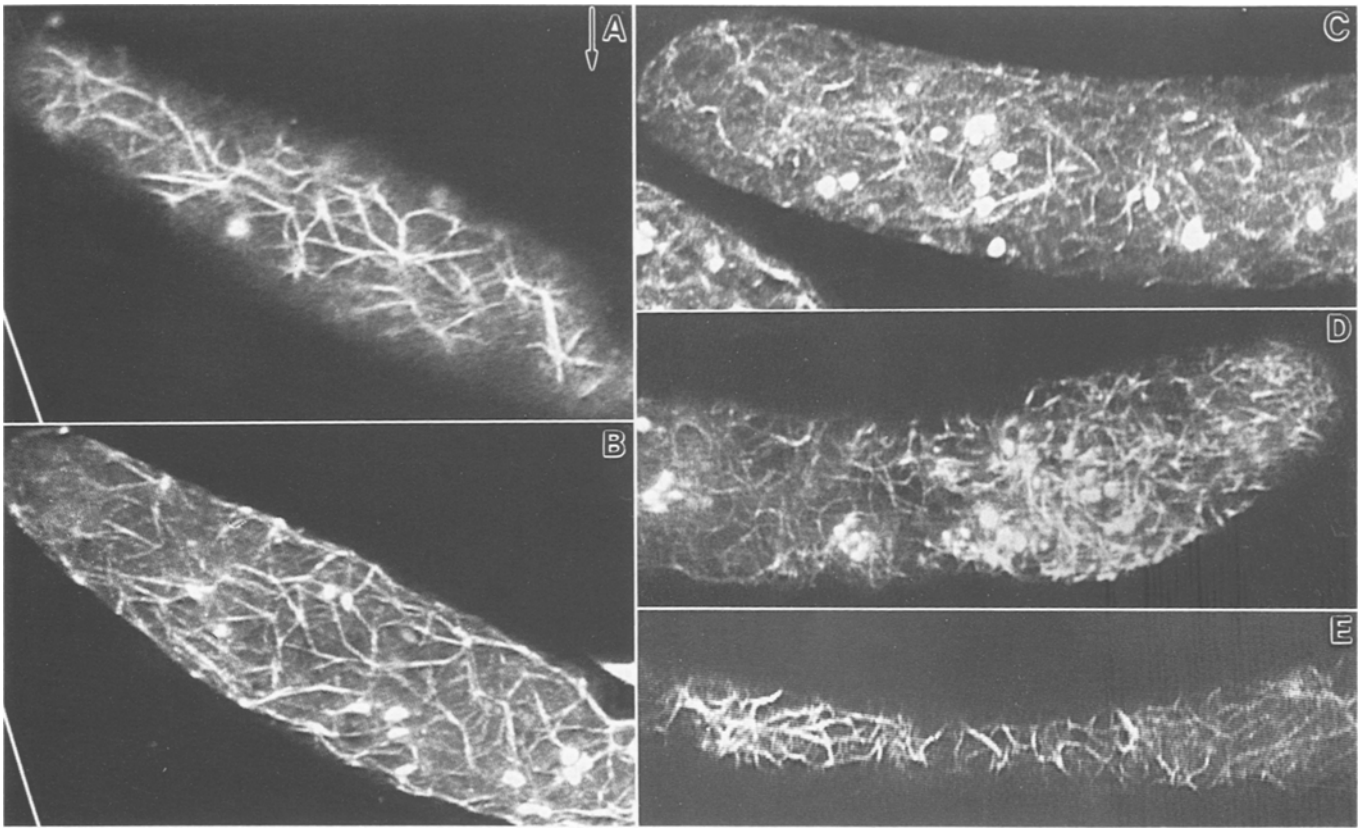

Fig. 5. Rhodamine phalloidin labelling of microfilaments in three different gravistimulated protonemata. Protonemata were kept horizontal for 3 h and observed using confocal laser scanning microscopy. Arrow in **A** indicates direction of gravity vector for **A–E**. **A** and **B** Two different optical sections of the same apical cell demonstrating peripheral (**A**) and more internal (**B**) microfilaments. Protonema tip is towards the upper left. Note upward curvature. ×1500. **C** Near median optical section of apical cell. Tip is to the left. ×1250. **D** Apical cell. Note abundant microfilaments in the extreme apex (upper right). ×1250. **E** Subapical cell. ×800

Discussion

Optimal techniques for microfilament visualization

MBS pretreatment and rhodamine phalloidin (MBS/RP) staining produced the best localization of microfilaments in *Ceratodon* protonemata. Attempts to include a paraformaldehyde fixation step after MBS pretreatment led to a substantial loss of microfilaments. This result confirms previous reports that the use of MBS/RP without PFA fixation preserves finer microfilaments (Goodbody and Lloyd 1990, Cho and Wick 1991).

In *Ceratodon* protonemal cells observed with conventional microscopy, rhodamine phalloidin and immunofluorescence seemed to label different F-actin arrays. A dense, complex array of microfilaments was observed more often with rhodamine phalloidin, while axially oriented microfilaments were more conspicuous using immunofluorescence. Rhodamine phalloidin labelled many non-axial peripheral microfilaments and this might reduce the prominence of axial microfilaments present within the apical cell. Alternatively, the axial microfilaments might be an artifact, since immunofluorescence requires harsher processing than RP. However, it cannot be ruled out that the antibody is labelling a population of microfilaments (thick, axially oriented) not detected with rhodamine phalloidin.

Microfilament distribution in Ceratodon and comparison with other tip-growing cells

Dark-grown *Ceratodon* protonemata contain an extensive network of actin microfilaments. In general, denser and more complex microfilament arrays have been observed in moss and fern protonemata (Kadota and Wada 1989, Abel et al. 1989, Quader and Schnepf 1989, Tewinkel et al. 1989) than in other tip-growing

cells such as pollen tubes (Heslop-Harrison and Heslop-Harrison 1992), root hairs (Lloyd et al. 1987), algal rhizoids (Sievers et al. 1991), and fungal hyphae (Harold and Harold 1992, Jackson and Heath 1993). In tip-growing cells other than protonemata, microfilament arrays are often described as net-axial in orientation (Lloyd et al. 1987, Tiwari and Polito 1988, Pierson et al. 1989, Jackson and Heath 1993).

In *Ceratodon*, CLSM reveals that microfilaments are not simply in a net axial orientation, but clearly exist in a fine meshwork of microfilaments that are oriented in a complex fashion. Extensive arrays of microfilaments have also been reported in protonemata of the mosses *Physcomitrella* and *Funaria* (Abel et al. 1989, Quader and Schnepf 1989, Tewinkel et al. 1989). However, the microfilaments within the apical dome were not well preserved or characterized in these mosses. In contrast, in *Ceratodon*, a very rich and complex network of microfilaments occurs in the apical dome and is one of the densest dome arrays reported for any tip-growing cell.

In *Ceratodon* protonemata, previous studies using cytoskeletal inhibitors suggest that microfilaments help maintain plastid zonation, while microtubules regulate the extent to which plastids sediment towards gravity (Schwuchow and Sack 1994). The abundant microfilaments around the plastids, particularly in the apical dome, lend additional support for the possible involvement of microfilaments in the regulation of plastid zonation.

Although there were numerous internal microfilaments, peripheral microfilaments were more abundant in *Ceratodon* protonemata, even using rhodamine phalloidin and CLSM. This appears to be a general observation for plant cells shown to contain both internal and peripheral microfilaments (Panteris et al. 1992, Cho and Wick 1991, Cleary et al. 1992). Some of these cells have large central vacuoles, and most microfilaments would be expected to be located in the peripheral cytoplasm. However, in non-vacuolated regions of protonemata, peripheral microfilaments were also more abundant than internal microfilaments. Peripheral microfilaments might also appear more numerous if they were more readily preserved than internal microfilaments, e.g., because peripheral microfilaments might be stabilized by association with other structures such as cortical endoplasmic reticulum or the plasma membrane.

In *Ceratodon*, upward gravitropic curvature was associated with a microtubule enrichment near the lower flank, 10–25 μm behind the apex (Schwuchow et al. 1990). Serial optical sections of *Ceratodon* apical cells did not reveal a major redistribution of microfilaments in gravistimulated protonemata in any part of the apical cell, including the area where microtubule enrichment is known to occur. It is not possible to determine whether a subtle redistribution of microfilaments occurs since plastid movement takes place during processing. The movement of plastids in *Ceratodon* during pretreatment with MBS suggests that it is not a general fixative, although it is effective in crosslinking F-actin.

In summary, this study shows the presence of an extensive microfilament array in the apical dome and throughout the *Ceratodon* apical cell, and the absence of any major redistribution of microfilaments during gravitropism. It documents perhaps the most extensive F-actin network visualized in any tip-growing cell.

Acknowledgements

This work was supported in part by a NASA Graduate Student Researchers Program grant (LMW) and by NASA Space Biology grants NAGW-780 and NAG10-0085 (FDS).

References

Abel WO, Knebel W, Koop HU, Marienfeld JR, Quader H, Reski R, Schnepf E (1989) A cytokinin-sensitive mutant of the moss, *Physcomitrella patens*, defective in chloroplast division. Protoplasma 152: 1–13

Cho SO, Wick SM (1991) Actin in the developing stomatal complex of winter rye: a comparison of actin antibodies and Rh-phalloidin labeling of control and CB-treated tissues. Cell Motil Cytoskeleton 19: 25–36

Cleary AL, Gunning BE, Wasteneys GO, Hepler PK (1992) Microtubule and F-actin dynamics at the division site in living *Tradescantia* stamen hair cells. J Cell Sci 103: 977–988

Doonan JH, Cove DJ, Lloyd CW (1988) Microtubules and microfilaments in tip growth: evidence that microtubules impose polarity on protonemal growth in *Physcomitrella patens*. J Cell Sci 89: 533–540

Goodbody KC, Lloyd CW (1990) Actin filaments line up across *Tradescantia* epidermal cells, anticipating wound-induced division planes. Protoplasma 157: 92–101

Goode JA, Alfano F, Stead AD, Duckett JG (1993) The formation of aplastidic abscission (tmema) cells and protonemal disruption in the moss *Bryum tenuisetum* Limpr. is associated with transverse arrays of microtubules and microfilaments. Protoplasma 174: 158–172

Harold RL, Harold FM (1992) Configuration of actin microfilaments during sporangium development in *Achyla bisexualis*: comparison of two staining protocols. Protoplasma 171: 110–116

Harper JDI, McCurdy DW, Sanders MA, Salisbury JL, John PCL (1992) Actin dynamics during the cell cycle in *Chlamydomonas reinhardtii*. Cell Motil Cytoskeleton 22: 117–126

Heslop-Harrison Y, Heslop-Harrison J (1992) Germination of monocolpate angiosperm pollen: evolution of the actin cytoskeleton and wall during hydration, activation and tube emergence. Ann Bot 69: 385–394

Jackson SL, Heath IB (1993) The dynamic behavior of cytoplasmic F-actin in growing hyphae. Protoplasma 173: 23–34

Kadota A, Wada M (1989) Circular arrangement of cortical F-actin around the subapical region of a tip-growing fern protonemal cell. Plant Cell Physiol 30: 1183–1186

Lessard JL (1988) Two monoclonal antibodies to actin: one muscle selective and one generally reactive. Cell Motil Cytoskeleton 10: 349–362

Liu B, Palevitz BA (1992) Organization of cortical microfilaments in dividing root cells. Cell Motil Cytoskeleton 23: 252–264

Lloyd CW, Pearce KJ, Rawlins DJ, Ridge RW, Shaw PJ (1987) Endoplasmic microtubules connect the advancing nucleus to the tip of legume root hairs, but F-actin is involved in basipetal migration. Cell Motil Cytoskeleton 8: 27–36

Panteris E, Apostolakos P, Galatis B (1992) The organization of F-actin in root tip cells of *Adiantum capillus veneris* throughout the cell cycle: a double label fluorescence microscopy study. Protoplasma 170: 128–137

Parthasarathy MW, Perdue T, Witztum A, Alvernaz J (1985) Actin network as a normal component of the cytoskeleton in many vascular plant cells. Amer J Bot 72: 1318–1323

Pierson ES, Kengen HMP, Derksen J (1989) Microtubules and actin filaments co-localize in pollen tubes of *Nicotiana tabacum* L. and *Lilium longiflorum* Thunb. Protoplasma 150: 75–77

Quader H, Schnepf E (1989) Actin filament array during side branch initiation in protonema cells of the moss *Funaria hygrometrica*: an actin organizing center at the plasma membrane. Protoplasma 151: 167–170

Schwuchow J, Sack FD (1994) Microtubules restrict plastid sedimentation in protonemata of the moss *Ceratodon*. Cell Motil Cytoskeleton 29: 366–374

– – Hartmann E (1990) Microtubule distribution in gravitropic protonemata of the moss *Ceratodon*. Protoplasma 159: 60–69

Seagull RW, Falconer MM, Weerdenburg CA (1987) Microfilaments: dynamic arrays in higher plant cells. J Cell Biol 104: 995–1004

Sievers A, Kramer-Fischer M, Braun M, Buchen B (1991) The polar organization of the growing *Chara* rhizoid and the transport of statoliths are actin-dependent. Bot Acta 104: 103–109

Sonobe S, Shibaoka H (1989) Cortical fine actin filaments in higher plant cells visualized by rhodamine-phalloidin after pretreatment with m-maleimidobenzoyl N-hydroxysuccinimide ester. Protoplasma 148: 80–86

Steer MW, Steer JM (1989) Pollen tube tip growth. New Phytol 111: 323–358

Tang X, Lancelle SA, Hepler PK (1989) Fluorescence microscopic localization of actin in pollen tubes: comparison of actin antibody and phalloidin staining. Cell Motil Cytoskeleton 12: 216–224

Tewinkel M, Kruse S, Quader H, Volkmann D, Sievers A (1989) Visualization of actin filament pattern in plant cells without pre-fixation: a comparison of differently modified phallotoxins. Protoplasma 149: 178–182

Tiwari SC, Polito VS (1988) Organization of the cytoskeleton in pollen tubes of *Pyrus communis*: a study employing conventional and freeze-substitution electron microscopy, immunofluorescence, and rhodamine-phalloidin. Protoplasma 147: 100–112

Walker LM, Sack FD (1990) Amyloplasts as possible statoliths in gravitropic protonemata of the moss *Ceratodon purpureus*. Planta 181: 71–77